PHYSICAL REVIEW A VOLUME 46, NUMBER 3 1 AUGUST 1992

Coupled-mode analysis of the self-induced-transparency soliton switch

A. Guzman
Departamento Fisica, Universidad Nacional de Colombia, Bogota, Colombia

F. S. Locati, M. Romagnoli, and S. Wabnitz
Fondazione Ugo Bordoni, via B. Castiglione 59, 00142 Roma, Italy
(Received 25 July 1991)

The dynamics of a nonlinear resonant tapered coupler is analyzed by using coupled-mode equations. The constituent waveguides are made of a linear host material doped with resonant impurities. Such a system allows a mechanism for all-optical switching. It is shown that nonlinear exchange between coupled waveguides originates from the group-velocity dependence on the propagating pulse power and/or area. The transmitted signal is always a multiple of the self-induced-transparency fundamental soliton. The dynamics of the pulse tuned or detuned from the resonance and with the inclusion of the material relaxation terms is discussed. In the last section the problem of soliton collision in the coupling region is considered; in this case an initial interpulse phase difference may determine a power-dependent outport switching.

PACS number(s): 42.50.Rh, 42.65.Pc, 42.79.Gn

I. INTRODUCTION

Accomplishment of extremely high-speed transmission and all-optical signal processing are main goals in integrated-optics research. Nonlinear phenomena are of great potential in this context, since they give rise to intensity-dependent propagation features. Effects of nonresonant nonlinearities on pulse propagation and directional couplers, such as those due to the intensity dependence of the refractive index in Kerr-type media, have been extensively investigated [1]. Once the nonlinearity counterbalances exactly the pulse temporal broadening due to group-velocity dispersion, the ultrashort pulse propagating through a Kerr-type medium is transformed into a soliton [2]. By exploiting the particlelike nature of solitons, it has been demonstrated that power-dependent nonlinear switching in bidirectional devices shows an extinction ratio equal to 1 [3,4]. Despite this improvement, the power threshold for soliton switching is still high. In contrast to Kerr-type nonlinear media, there are resonant systems that provide large nonlinearities, but these media are saturation limited and slow in the thermalization process. The switching performance of a nonlinear directional coupler (NLDC) incorporating a medium with a two-level saturable nonlinearity has already been analyzed [5]. Coherent pulse propagation through resonant media is known to have a soliton propagation regime, a phenomenon that is called self-induced transparency (SIT) [6]. This phenomenon increased interest in switching applications because of the combined effect of absence of absorption loss and maximum nonlinear efficiency attainable from a two-level system. Analogous to Kerr-type soliton switching, it has been demonstrated [7] that, with the coupled-mode approach, the SIT soliton switching in NLDC is possible. In this case the extinction ratio of the NLDC is equal to 1 as for the case of Kerr soliton switching, while the power requirement to reach the switching threshold decreases as the dipole moment of the two-level transition increases. The theory of SIT soliton propagation holds only for plane and spatially uniform waves; in fact, experiments performed with Gaussian beams in two-level system materials have shown that the soliton propagation is unstable [8]. Conversely, when the pulse is confined in a guiding structure, the diffraction is compensated [9,10] and the scalar approach adopted previously either for the single-channel waveguide or for the NLDC [7] is shown to be valid. The possibility of inducing self-transparency has been recently proposed for excitons in semiconductors. Zero-dimensional bound excitons trapped by impurities, as well as two-dimensional excitons in quantum wells, can be considered as static "two-level atoms" with large dipole moments and long decay times [11]. As an alternative to the saturable or Kerr-type nonlinear coupler, here we analyze in detail the switching properties of pulses propagating in a coherent regime through a nonlinear resonant coupler, whose constituent waveguides are made of a linear host material doped with resonant impurities. As an example, we consider the above-mentioned bound excitons in semiconductors as resonant impurities. For the sake of simplicity, they are modeled as homogeneously broadened two-level systems with energy levels on and off resonance with the guided light frequency. The total medium polarization also includes a nonresonant contribution originating from the host material which determines the guiding properties of the waveguide. We apply the technique of coupled-mode expansion, including the resonant polarization as source term of a generalized set of Maxwell-Bloch equations. The theory of self-induced transparency assumes a frozen two-level system and therefore discards all terms containing relaxation times. In this work, the influence of relaxation times on the output channel discrimination of the NLDC has been evaluated. This permits us to establish the upper limit of pulse duration chosen for the switching process. In addition to single-pulse self-switching, gating a signal pulse with another pulse traveling on the cross channel of the bidirectional device may be useful for optical logic operations. Gating a pulse with another pulse, applied to the case of coherent propagation and therefore to SIT soliton interaction in the coupling region of the NLDC, has provided further insights to the mechanism of SIT soliton switching. In Sec. IV it is shown that two SIT solitons independently launched into the two inputs ports of the NLDC join into one of the two channels if there exists an interpulse phase difference different from a multiple of π. The amount of phase difference determines the threshold of gating and the sign of the difference, the output channel.

II. COUPLED-MODE FIELD EQUATIONS WITH A RESONANT POLARIZATION

A dual-channel directional coupler consists of two dielectric waveguides placed close enough together to be coupled through the evanescent fields. We consider here a type of nonlinear resonant coupler whose constituent waveguides contain impurities which can be described as a two-level system. Propagation of light pulses through the coupler is described by the wave equation

$$\nabla^2 \mathbf{E}(\mathbf{r},t)=\mu\varepsilon_0 \frac{\partial^2}{\partial t^2}\mathbf{E}(r,t)+\mu\frac{\partial^2}{\partial t^2}\mathbf{P}'(\mathbf{r},t) , \tag{1}$$

where $\mathbf{E}(\mathbf{r},t)$ is the pulse electric field and $\mathbf{P}'(\mathbf{r},t)$ is the total medium polarization which includes host as well as contributions:

$$\mathbf{P}'(\mathbf{r},t)=\mathbf{P}'_0(\mathbf{r},t)+\mathbf{P}'_{\text{imp}}(\mathbf{r},t) . \tag{2}$$

Since we are dealing with the nonlinearity caused by the impurities alone, the waveguide acts only as a supporting medium and

$$\mathbf{P}'_0(\mathbf{r},t)=[\epsilon(\mathbf{r})-\epsilon_0(\mathbf{r})]\mathbf{E}(\mathbf{r},t)$$

is the waveguide polarization matrix induced by $\mathbf{E}(\mathbf{r},t)$, $\epsilon(\mathbf{r})$ is the dielectric constant of the directional coupler, and $\mathbf{P}'_{\text{imp}}(\mathbf{r},t)$ stands for the induced resonant impurity polarization. The equation for the slowly varying approximation of the field $\mathbf{E}(\mathbf{r},t)$ and the polarization $\mathbf{P}(\mathbf{r},t)$ reads

$$\begin{aligned}2\beta\left[\frac{\partial}{\partial z}+\beta'\frac{\partial}{\partial t}\right]\mathbf{E}(\mathbf{r},t) &= -i\left[\beta^2-\frac{\omega^2}{c^2}n^2(\mathbf{r})\right]\mathbf{E}(\mathbf{r},t)\\ &\quad +i\nabla_T^2\mathbf{E}(\mathbf{r},t)+i\mu_0\omega^2\mathbf{P}'(\mathbf{r},t) .\end{aligned} \tag{3}$$

Here β is the linear propagation constant of the waveguide mode, $1/\beta'=(c/n^2)(\beta/k)$ is the mode group velocity, and $n(\mathbf{r})$ is the linear index of refraction and contains the index profile of the coupler. Equation (3), together with the equations governing the evolution of the two-level system, which will be shown later, represent a complete set which is able to describe the coherent propagation regime. In the uniform plane-wave case and assuming a homogeneous medium, Eq. (3) may be solved without the diffractive terms and a possible solution concerns the case of solitary-wave propagation [6]. This approach lacks validity in real situations where the light beams are transversally limited [8]; in fact, the diffractive spreading of the pulse inhibits any stationary behavior of the traveling soliton. The confinement of the radiation in a guiding structure may compensate for the longitudinal instability caused by diffraction; it has been shown [10] that a pulse with an amplitude and a duration satisfying the uniform plane-wave case may propagate, in the regime of self-induced transparency, in waveguides as well. The only assumption required to obtain the equivalency of the two cases is that the impurity doping profile has to match the index profile of the waveguide. By applying the same considerations to the problem of the directional coupler, it has been found that the equivalency between the solution obtained in the coupled-mode approach [7] and the exact one [10] deduced from Eq. (3), still exists. In the course of the discussion, in order to go through the physical nature of the switching process, we will adopt the coupled-mode approach. To develop a coupled-mode theory, we expand the total field in terms of the modes of the isolated constituent waveguides. For the sake of simplicity we consider single-mode waveguides with the field propagating along the z axis and we ignore coupling to the continuum of radiation modes; the expression of the electric field is

$$\mathbf{E}(\mathbf{r},t)=\frac{1}{2}\sum_{j=1}^{2}\{e_j E_{0j}(z,t)\phi_j(x,y)\exp[i(\beta_j z-\omega t)]+\text{c.c.}\} . \tag{4}$$

In Eq. (4), the index j labels the waveguides, $\mathbf{e}_j$ are unit vectors indicating the light polarization, β_j are propagation constants, and ω is the frequency of the carrier wave. $E_{0j}(z,t)$ are slowly varying complex amplitudes of the fields and $\phi_j(x,y)$ are normalized mode functions that determine the transverse distribution of the electric field in the waveguides. They are obtained by solving the corresponding boundary-value problem for each specific waveguide structure, and satisfy

$$\left[\frac{\partial^2}{\partial x^2}+\frac{\partial^2}{\partial y^2}+\frac{\omega^2}{c^2}n_j^2(\mathbf{r})-\beta_j^2\right]\phi_j(x,y)=0 , \tag{5}$$

where $\epsilon_j(\mathbf{r})=n_j^2(r)\epsilon_0$ is the dielectric constant of the isolated j waveguide. The induced resonant polarization can also be expanded in terms of its slowly varying complex amplitudes $P_{0j}(\mathbf{r},t)$ namely,

$$\mathbf{P}'_{\text{imp}}(\mathbf{r},t)=\frac{1}{2}pN_{\text{imp}}\sum_{j=1}^{2}\{\mathbf{e}_j P_{0j}(\mathbf{r},t)\exp[i(\beta_j z-\omega t)]+\text{c.c.}\} , \tag{6}$$

where N_{imp} is the impurity concentration and $p=\langle a|\mathbf{p}\cdot\mathbf{e}|b\rangle$ is the dipole matrix element. Substitution of Eqs. (2), (4), and (6) into the wave equation (3), together with Eq. (5), leads to first-order partial differential equations for the slowly varying field amplitudes. If the linear dispersion spreading caused by the waveguide matrix in the short distance traveled by the fields through the directional coupler is negligible, the slowly varying approximation can be applied for both $E_{0j}(z,t)$ and $P_{0j}(\mathbf{r},t)$ to obtain

$$\sum_j \left\{ \left[\beta_j \left[\frac{\partial E_{0j}}{\partial z} + \beta_j' \frac{\partial E_{0j}}{\partial t} \right] + \frac{i}{2}\frac{\omega^2}{c^2}[n^2(\mathbf{r}) - n_j^2(\mathbf{r})]E_{0j} \right] \phi_j \exp[i\beta_j z - \omega t] + \text{c.c.} \right\}$$
$$= i\mu p N_{\text{imp}} \omega^2 \sum_{j=1}^{2} \{ P_{0j}(\mathbf{r},t)\exp[i(\beta_j z - \omega t)] + \text{c.c.} \} . \quad (7)$$

Coupled-mode field equations are derived from Eq. (7) by multiplying both sides by $\phi(x,y)$ and integrating over the coupler cross section. For simplicity we consider a symmetric coupler consisting of two identical waveguides, where phase mismatch effects are avoided, and we assume the same polarization for the guided fields. Therefore, we omit the waveguide subindex wherever it is not required, obtaining

$$\sum_{j=1}^{2} \left[\frac{\partial E_{0j}}{\partial z} S_{jl} + \frac{k}{\beta c}\frac{\partial E_{0j}}{\partial t} N_{jl} - \frac{i}{2}\frac{k^2}{\beta} E_{0j} K_{jl} \right] = \frac{i}{2}\frac{k^2 p N_{\text{imp}}}{\beta \epsilon_0} \sum_{j=1}^{2} \langle P_{0j} \rangle_l , \quad l = 1,2 \quad (8)$$

where $k = \omega / c$. In the left-hand side we have introduced the matrices

$$S_{jl} \equiv \int dx \int dy\, \phi_j(x,y)\phi_l(x,y) \Big/ \int dx \int dy\, \phi_j^2(x,y) ,$$
$$N_{jl} \equiv \int dx \int dy\, n^2(\mathbf{r})\phi_j(x,y)\phi_l(x,y) \Big/ \int dx \int dy\, \phi_j^2(x,y) , \quad (9)$$
$$K_{jl} \equiv \int dx \int dy [n_j^2(\mathbf{r}) - n^2(\mathbf{r})]\phi_j(x,y) \times \phi_l(x,y) \Big/ \int dx \int dy\, \phi_j^2(x,y) ,$$

where again $n^2(\mathbf{r}) = \epsilon(\mathbf{r})/\epsilon_0$ is the nonresonant index of refraction of the directional coupler. $\mathbf{S}$ is a normalized mode overlap matrix whose diagonal elements are equal to 1. The diagonal elements of $\mathbf{N}$ represent the average $\langle n^2(\mathbf{r}) \rangle$ over the waveguide cross section. The value of the $\mathbf{K}$ matrix elements depends on the penetration of the evanescent wave of one guide into the other, and is responsible for the waveguide coupling, as will be shown below. The source term at the right-hand side of Eq. (8) is a cross-section-averaged resonant polarization $\langle P_{0j}(x,y,t) \rangle$ defined as

$$\langle P_{0j}(x,y,t) \rangle_l = \int dx \int dy\, P_{0j}(x,y,t)\phi_l(x,y) \Big/ \int dx \int dy\, \phi_l^2(x,y) . \quad (10)$$

Further simplification of Eq. (8) is obtained by assuming weak coupling and neglecting terms of the normalized overlap matrix element S_{12} which are small compared to 1:

$$\frac{\partial E_{0j}}{\partial z} + \frac{1}{v}\frac{\partial E_{0j}}{\partial t} - imE_{0j} - i\kappa E_{0l} = \frac{ikpN_{\text{imp}}}{2\beta\epsilon_0} \langle P_{0j} \rangle_j , \quad j = 1,2 \;\; l \neq j . \quad (11)$$

The constants $1/v = k\langle n^2(\mathbf{r}) \rangle / (\beta c)$, which is $\langle \beta' \rangle$, and $\kappa = k^2 K_{12}/(2\beta)$ in Eq. (11) represent an effective group velocity and the evanescent coupling strength between the two waveguides. The field term multiplied by the constant $m = k^2 K_{jj}/(2\beta)$ introduces a phase which can be easily transformed out and will not be considered further. In our model, the sources of the resonant polarization are waveguide impurities, which behave like homogeneously broadened two-level systems driven by the guided field. The corresponding density-matrix equations in the interaction picture read [7]

$$\frac{\partial}{\partial t} P_{0j} = -(\gamma_2 - i\Delta)P_{0j} + i\frac{p}{2\hbar}\phi_j E_{0j} W_{0j} ,$$
$$\frac{\partial}{\partial t} W_{0j} = -\gamma_1 (W_{0j} - W_{0j}^{\text{eq}}) + i\frac{p}{\hbar}\phi_j (E_{0j}^* P_{0j} - E_{0j} P_{0j}^*), \quad (12)$$

where $\Delta = \omega_0 - \omega$ is the field frequency detuning from resonance; $\hbar\omega_0 = E_a - E_b$ is the resonant transition energy between the atomic eigenstates $|a\rangle$ and $|b\rangle$; $pE_{0j}(z,t)/\hbar$ is the Rabi frequency; and γ_1 and γ_2 are, respectively, the longitudinal and transverse relaxation rates of the two-level systems. The induced resonant polarization expressed in Eq. (2) is related to the density matrix through $P'_{\text{imp}}(\mathbf{r},t) = N_{\text{imp}}\text{Tr}(\mathbf{P}\mathbf{p})$, where $\mathbf{P}$ is the complete density matrix containing P_0, W_0, and the difference of population at the equilibrium, $W_0^{\text{eq}} = 1$. Then, the source term in the field equation (11) is given by

$$\langle P_{0j}(x,y,t) \rangle_j = \int dx \int dy\, P_{0j}(x,y,t)\phi_j(x,y) \Big/ \int dx \int dy\, \phi_j^2(x,y) , \quad (13)$$

where again the spatial average of the density-matrix elements over the coupler cross section is involved. Since our coupled-mode theory is based on the assumption that the transverse structure of the fields in the waveguides is determined by the guiding properties of the host material and is not affected by the nonlinear interaction with the resonant impurities, the density-matrix elements are assumed to have the same transverse structure [10] of the guided mode when averaging them in Eqs. (12) and (13). The first assumption is valid only for low doping concentrations since, in principle, the density-matrix elements in Eqs. (12) are nonlinear functions of the field and therefore their transverse and temporal dependence cannot be separated. Our averaging procedure imposes the linear waveguide structure over the nonlinear dynamics. For large impurity densities the mode structure would be affected and results of the coupled-mode approach would be invalid. To perform the spatial average, we integrate Eqs. (12) over the coupler cross section, and there, as well as in Eq. (13), we do the replacement

$$\begin{aligned} P_{0j}(\mathbf{r},t) &= P_j(x_0,y_0,z,t)\phi_j(x,y) , \\ W_{0j}(\mathbf{r},t) - W_{0j}^{\mathrm{eq}}(\mathbf{r},t) &= [W_j(x_0,y_0,z,t) - W_j^{\mathrm{eq}}(x_0,y_0,z,t)]\phi_j(x,y) , \quad j=1,2 . \end{aligned} \tag{14}$$

The pair (x_0,y_0) represents the transverse coordinates of the maximum of the function $\phi(x,y)$. It can be easily seen from Eqs. (13) and (14) that $P_j(x_0,y_0,z,t)$ is proportional to the average source polarization $\langle P_{0j}\rangle_j = N_{\mathrm{imp}} p P_j$. The quantity $W_j(x_0,y_0,z,t)$ instead is the population inversion between levels $|b\rangle$ and $|a\rangle$ at the peak of the distribution $\phi(x,y)$. The averaged equations (12) represent the motion equations for the variables P_j and W_j, which together with the coupled-mode field equations (11) constitute the following generalized system of Maxwell-Bloch equations for the nonlinear directional coupler:

$$\begin{aligned} \frac{\partial}{\partial t'} P_j &= -(\gamma_2' - i\Delta')P_j + \frac{i}{2} U_j W_j , \\ \frac{\partial}{\partial t'} W_j &= -\gamma_1'(W_j - W_j^{\mathrm{eq}}) + i(U_j^* P_j - P_j^* U_j) , \\ \frac{\partial U_j}{\partial z'} + \frac{1}{V}\frac{\partial U_j}{\partial t'} - iKU_l &= iP_j, \quad j,l=1,2, \quad l\neq j . \end{aligned} \tag{15}$$

The set of equations (15) has been reduced to a dimensionless form through the following substitutions: $U_j = \mathcal{F} p \tau_0 E_{0j} \hbar^{-1}$, which is the field in area units, with τ_0 an arbitrary pulse width; the quantities $t' = t(\tau_0)^{-1}$, $z' = \alpha' \tau_0 z$, $\gamma_1' = \gamma_1 \tau_0$, $\gamma_2' = \gamma_2 \tau_0$, $\Delta' = \tau_0 \Delta$, $V = \alpha' v \tau_0^2$, $K = \mathcal{F} k (\alpha' \tau_0)^{-1}$, and

$$\alpha' = \mathcal{F} N_{\mathrm{imp}} k^2 p^2 (2\hbar\beta\epsilon_0)^{-1}$$

are also expressed in dimensionless units. The form factor $\mathcal{F}$ derives from the average integrals and is defined as

$$\mathcal{F} = \int dx \int dy\, \phi_j^3(x,y) \Big/ \int dx \int dy\, \phi_j^2(x,y) ,$$

which depends on the specific mode structure of the waveguide. This is of the order of 1 for the TE mode of a planar waveguide. The coefficient α' is proportional to the absorption coefficient of the resonant impurities [12]; K is the normalized linear coupling constant of the directional coupler. In the absence of the nonlinear resonant polarization, K determines the normalized coupling length $l = \pi(2K)^{-1}$ for which complete power transfer between the waveguides takes place. The system of equations (15) was solved numerically in a moving reference frame defined by the coordinate $\zeta = (z' - Vt')$ by assuming swept excitation of the resonant impurities.

III. RESONANT SOLITON SWITCHING

From the self-induced-transparency equations (15) in the zero detuning case ($\Delta = 0$) and for pulse durations much shorter than relaxation times ($\gamma_1 = \gamma_2 = 0$), one can obtain two coupled sine-Gordon equations that read

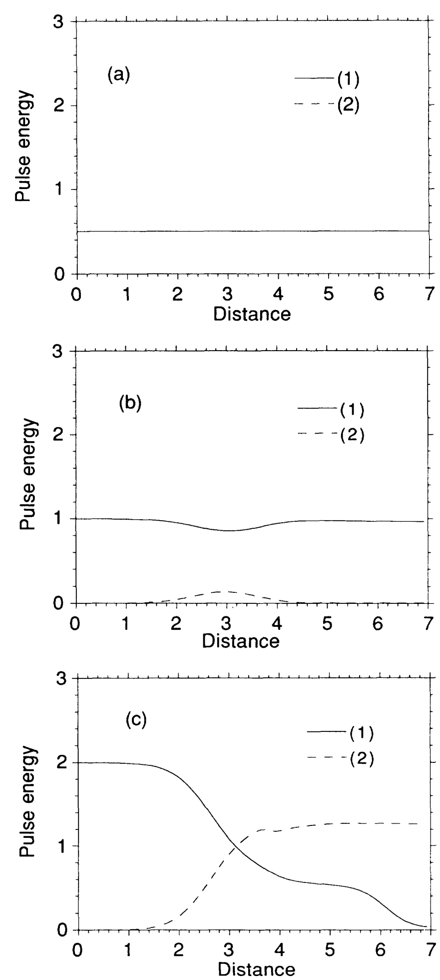

FIG. 1. Energy evolution vs distance ζ of three different 2π solitons: (a) $A = 0.25$, $\tau' = 4$; (b) $A = 0.5$, $\tau' = 2$; and (c) $A = 1$, $\tau' = 1$, through the dual-channel directional coupler whose parameters are $K = 2$, $d = 1$, $\zeta_m = 3$, $\zeta_{\mathrm{out}} = 7$. The solid and dashed curves correspond respectively to the bar (1) and cross (2) channels of the NLDC. The curve relative to the cross channel in (a) coincides with the abscissa.

$$\frac{\partial^2 \psi_1}{\partial \zeta \partial t'} = \sin\psi_1 - K\frac{\partial \psi_2}{\partial t'} ,$$
$$\frac{\partial^2 \psi_2}{\partial \zeta \partial t'} = \sin\psi_2 - K\frac{\partial \psi_1}{\partial t'} , \quad (16)$$

where

$$\psi_j(t') = \int_{-\infty}^{t'} U_j(t'')dt''$$

is, in the limit of $t' = \infty$, the definition of the pulse area. Without the evanescent field coupling term ($K = 0$), the two equations become independent and both show steady-state solutions in the form of kinks [6] whose pulse areas are equal to an integer multiple of 2π. The same happens to the asymptotic solutions for transmitted pulses in the NLDC if the evanescent coupling is localized, say, tapered couplers. Therefore, we assume a Gaussian function for the coupling coefficient (Ref. [13]) K in Eqs. (15) and (16), namely,

$$K = K_0 \exp[-(\zeta - \zeta_m)^2/2d^2] ,$$

where ζ_m and d are coupling parameters, with $d = \alpha'\tau_0 D$, where D is the tapering width in real units. Before the coupling starts acting, input pulses of arbitrary area evolve towards their nearest steady-state solution as $\exp(\pm\zeta)$ [6]. Excitation of the NLDC is done by injection of pulses

$$U_1(t') = A \operatorname{sech}[(t' - t'_0)/\tau']$$

into one waveguide. In the region of coupling the evolution of the injected pulse is governed by the balance of the terms in the right-hand sides of Eqs. (16). As an example, in the case of a 2π pulse the field is proportional to the inverse of the pulse duration; therefore, the second term in the right-hand side of Eqs. (16) is linearly proportional to the ratio K/τ' and gives rise to an effective coupling coefficient dependent on τ' of the corresponding injected pulse. This property allows different pulses to have different evolutions since in any case the sine term is limited in the range $(-1, +1)$ while the linear one may assume any value (this is done by varying τ'). This means

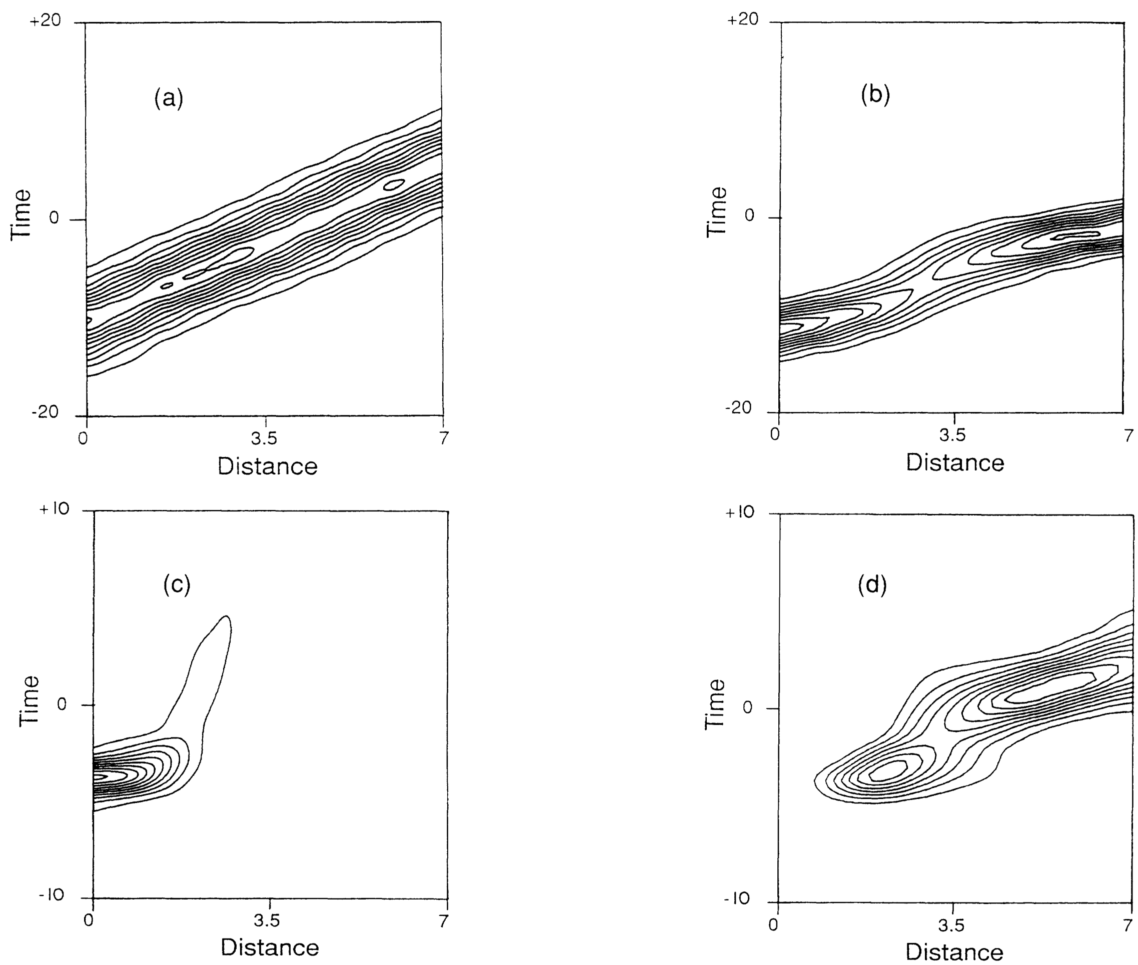

FIG. 2. Space-time maps representing the cases depicted in Fig. 1. The solitons travel with different envelope velocities; the faster they are, the greater is the coupling. In (a) and in (b) the evolution in the input channel is reported; in (c) the injected soliton velocity is closer than previously to the speed of the light, and the energy injected into the input channel is completely transferred into the cross channel (d). The horizontal axis is the distance ζ, and the vertical axis is the time t'.

that for a short pulse of area 2π, switching to the second guide is easily obtained whenever $\tau' \ll K$; for long pulses on the contrary, no transfer takes place even at higher powers ($\tau' \gg K$). In order to give a greater insight into the switching process, we studied numerically the transmission characteristics of the NLDC by varying the pulse duration, while keeping constant the product $A\tau'$ which is proportional to the pulse area. The values for the parameters are $K=2$, $\zeta_m=3$, $d=1$. In Fig. 1 the energy-evolution curves through the two arms of the directional coupler for an injected 2π pulse as a function of the pulse duration have been reported. The energy is defined as

$$N=\int_{-\infty}^{+\infty}|U_j(t')|^2dt' .$$

In Fig. 1(a), the input 2π pulse, with $A=0.25$ and $\tau=4$, flows through the coupling region and emerges entirely from the same guide; in this case no exchange is observed. In Fig. 1(b), $A=0.5$ and $\tau'=2$; a weak transfer through the region of coupling occurs, but it is not sufficient for a SIT soliton formation in the coupled waveguide; in Fig. 1(c), $A=1$ and $\tau'=1$; the input pulse is transmitted into the other arm of the NLDC, and no residual energy is left in the input channel. For the SIT solitons, changing τ' means an increase or a decrease of the envelope velocity too; in fact, a short soliton travels at most as fast at the speed of the light in the medium, while a long one may be orders of magnitude slower. In the following it is shown that the pulse envelope velocity determines the evolution of the 2π fundamental soliton with different pulse durations. In Fig. 2(a), $A=0.25$ and $\tau'=4$; the pulse travels much slower than the light in the medium. When it goes through the coupler, the coupled portion of energy is suddenly absorbed and no light emerges from the end of the coupled channel. In Fig. 2(b), $A=0.5$ and $\tau'=2$; a portion of energy is transferred into the second waveguide, but the correspondent area is below the threshold for stationary pulse formation. In this case more energy than previously is transferred, but the velocity of the coupled wave is quite different from that of the light and the absorption coefficient is such that the energy is absorbed before a consistent portion of energy arrives from the input channel. Of course, this is not true if the input pulse is fast enough. In Fig. 2(c), $A=1$ and $\tau'=1$; the transferred energy is above the threshold for soliton formation, no energy is left in the input channel, and the soliton is completely rebuilt in the second channel. A good tradeoff between the main parameters governing the switching process is obtained for $\tau'=K$. As an example, we show in Fig. 3 the transmission of hyperbolic secant pulses across the coupler as a function of their amplitude A. In the region where $A<0.3$, no soliton shows up because the associated area is too small; the doped waveguide acts as a resonant absorber with overall intensity losses. Therefore, after propagation over several absorption lengths, the pulse energy is completely absorbed. In the region where $0.3<A<0.6$, a 2π soliton is formed and, as outlined above, it also emerges from the same channel [as an example, see Fig. 2(a)]. For values of A between 0.6 and

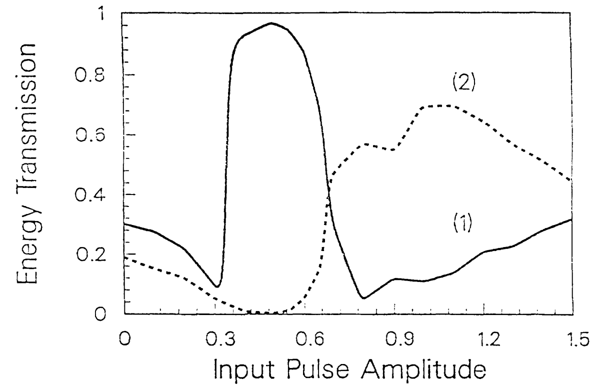

FIG. 3. Energy transmission normalized to the input energy for channels (1) and (2) as function of the amplitude A. The pulse was launched in channel (1) and the duration was $\tau'=2$. The parameters of the directional coupler are the same as those reported in Fig. 1.

1.2, only the second waveguide transmits power. In particular, as shown in Fig. 4, for $A=1$ a 4π soliton being coupled to the second channel breaks up into two 2π pulses, as expected from the evolution of the higher-order

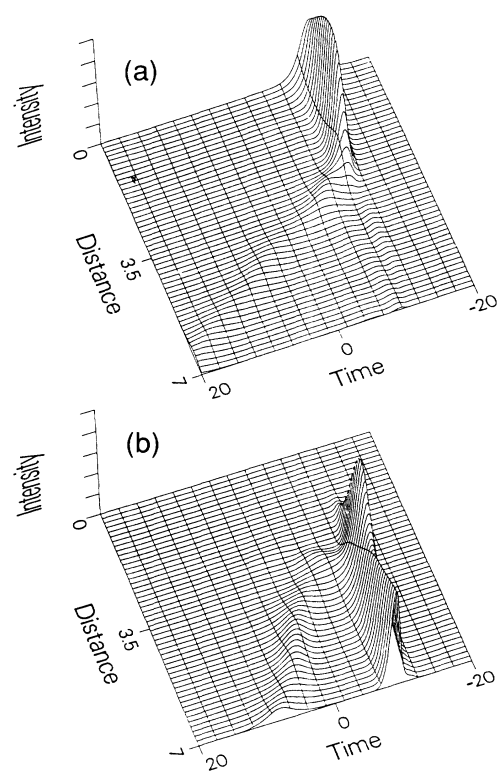

FIG. 4. Propagation of a 4π soliton through the directional coupler: $A=1$, $\tau'=2$. The energy injected into channel (1), in (a), is switched to the cross channel (2), in (b). Once the SIT soliton of order 2 (4π) is coupled into the crossed channel (2), it breaks up into two fundamental (2π) solitons whose amplitudes and durations are different. The parameters of the coupler are the same as those reported in Fig. 1. The intensity reported on the vertical axis corresponds to $|U_j|^2$ and is expressed in arbitrary units; the horizontal axes are propagation distance ζ and time t'.

solitons. In analogy, a threefold splitting is obtained when a 6π pulse is formed, but a pair of 2π pulses emerges from the coupled channel, while a single 2π pulse emerges from the input channel. For comparison, in Fig. 5 the transmission of the pulse area from the two arms of the NLDC is shown. It is worthwhile to note that when a 2π pulse propagates in the input channel without exchanging energy with the other, the area associated to the pulse is positive ($0.3 < A < 0.6$), while in case of coupling the areas change sign ($0.6 < A < 1.2$), as expected from the linear theory of coupling. For $A > 1.2$ even the pulse area emerging from the input waveguide is reversed in sign; this may suggest a double energy exchange in the coupling region. In any case, even though a higher-order soliton breaks up, the transmission of the coupler arms is always in multiples of fundamental solitons; in other words, the peculiarity of a SIT switch consists of digital transmission characteristics. Figures 3 and 5 should show, if evaluated at larger output distance ζ_{out}, better defined transmission regions with much steeper transitions as a function of A. Asymptotically, they should reflect the quantized switching properties of this NLDC, whereas either no intensity is transmitted or a definite number of solitons goes through. As an example for SIT soliton switching in a NLDC, we assume the bound excitons in CdS as resonant impurities [7,11]. In this case the relevant parameters in real units are $N_{imp} = 10^{19}$ m^{-3}, $\alpha' = 10$ cm^{-1} ps^{-1}, $\kappa = 10$ cm^{-1} (in the center of the tapered coupler), $z_{out} = 7$ mm, $D = 1$ mm, and $\tau = 2$ ps; to obtain a 2π soliton, we further assume a mode diameter of 2 μm. The resulting peak power is therefore 50 mW (an energy of 0.1 pJ), which demonstrates the potential of this mechanism for ultrafast switching. For comparison, the peak power requirement in the case of Kerr soliton switching [4] ranges from 1 to 7 kW depending on the choice of coupler length (1.8–0.45 m).

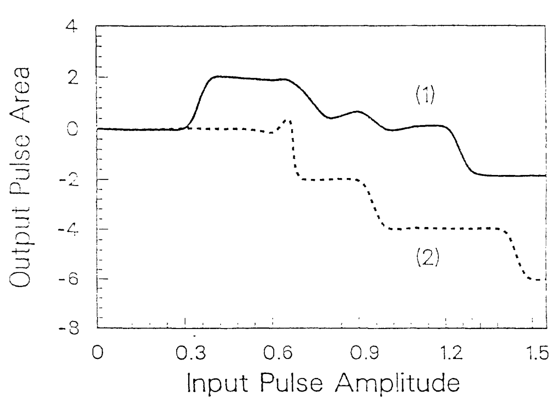

FIG. 5. Output pulse area vs input pulse amplitude for excitation of the NLDC on channel (1). The pulse was launched in channel (1) and the duration was $\tau' = 2$. The vertical axis is scaled in multiples of π. The area transmission exhibits a digital behavior. The coupler parameters are the same as those reported in Fig. 1.

IV. OFF-RESONANCE SOLITON SWITCHING

If the source is detuned from resonance, the set of equations (15) is fully involved; the term concerning the real part of the polarization generates a change of phase all along the propagating pulse. In this sense even though it has no meaning to consider further the evolution of the pulse area and indeed Eq. (16), most of the considerations discussed in the resonant case still apply. The polarization field originating from the light-matter interaction is reduced because of the off-resonance value of the susceptibility; therefore, the linear coupling term of the propagation in Eq. (15) may strongly affect the evolution of the injected pulse. In the following the same value for the coupling parameter ($K = 2$) will always be used and, since the absorption depends on the detuning Δ, the value of the absorption may always be maintained the same by compensating the decrease in absorption due

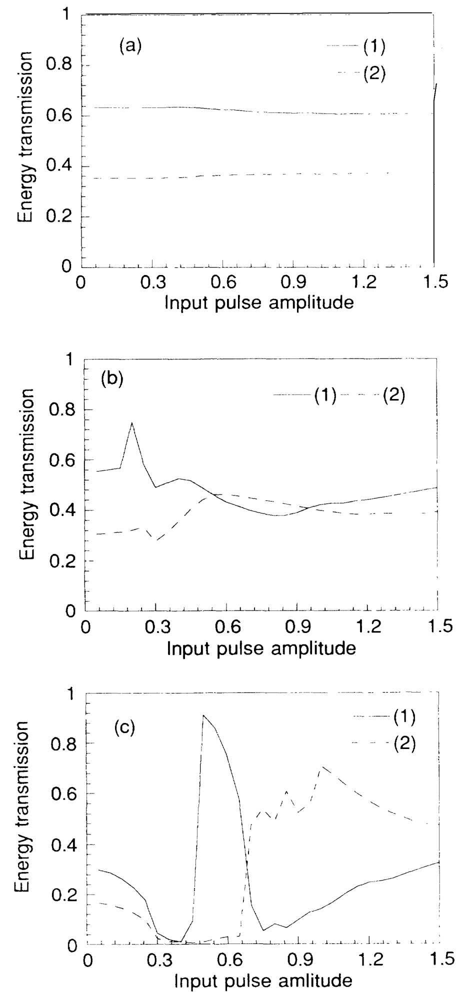

FIG. 6. Energy transmission normalized to the input energy as a function of the input amplitude A for the off-resonant case. Three different detunings are considered: (a) $\Delta = 1$, (b) $\Delta = 0.5$, and (c) $\Delta = 0.1$; for small detunings only the system acts as a SIT soliton switch, while for large detunings the device behaves linearly. The input pulse duration was $\tau' = 2$ and the coupler parameters are the same as those of Fig. 1.

to detuning with an increase of the impurity doping. In order to avoid overlapping with the problem of relaxation times, the material is assumed homogeneously broadened and the sharp line approximation is applied [14]. In particular, for τ' comparable with the shortest relaxation time, the same approximation applies, but large detunings are required. In any case, independently of the real value of the linewidth or of the relaxation times, the relevant factor for the discussion is $\Delta\tau'$. In Fig. 6 the NLDC power transmission at $\zeta_{out}=8$ is reported. In Fig. 6(a), $\Delta\tau'=1$; the device shows a flat dependence on the amplitude of the injected pulse. About 60% of the power emerges from the input channel and about 30% from the coupled channel. At this value of detuning the coupler is linear; the outcoming pulses are shaped similarly to those at the input because of the weak interaction through the off-resonance two-level system. In Fig. 6(b) the term $\Delta\tau'=0.5$; the SIT soliton evolution through the coupler as a function of the injected amplitude starts becoming closer to the resonant case. The low-amplitude side of the transmission shows an increase of energy exchange, even though the contrast between the transmitted powers is low, while the high-amplitude side of the curves looks like that of Fig. 6(a) because the velocity of the pulse envelopes of higher-order SIT solitons grows progressively larger and hence the linear coupling prevails. In Fig. 6(c), $\Delta\tau'=0.1$; the switching behavior resembles that of the resonant propagation case. For $A>0.4$, a 2π soliton starts growing; at $A\approx 0.5$ the transmission of the input waveguide is close to 1. By increasing the injected power, $0.6<A<0.7$, the transmission of the input waveguide goes to zero, while most of the power emerges from the coupled guide and a 2π soliton is formed. For higher amplitudes the contrast between the channels becomes weaker. It is noteworthy that the envelope velocity contains a scaling factor due to the detuning [12]. As an example, for the 2π pulse,

$$v^{-1}=nc^{-1}+\alpha'\tau^2\{2\pi[1+(\Delta\tau)^2]\}^{-1},$$

which introduces an increase of velocity v determining a shift of the threshold for switching towards the low-power side of Fig. 6(c); see for comparison the position of the threshold for the resonant case illustrated in Fig. 3. In general, the detuning from resonance reduces the nonlinear propagation to a power-dependent phase shifting which resembles more closely the Kerr instead of the coherent propagation; this shows that, in the cases reported here, the mechanism based on the change of group velocity is more efficient with respect to that based on the phase-velocity change.

V. RELAXATION TIMES

Up to now, only the range of pulse durations much shorter than any damping effect has been considered. The presence of these terms introduces a certain degree of incoherent loss that decreases the amplitude of the traveling envelope. Although the whole set of equations (15) is involved, the effect of the relaxation to the steady-state values of both the polarization and difference of population $[P(t=\infty)=0$ and $W(t=\infty)=W^{eq}]$ is assumed to be slow compared to the pulse duration and this is done in order to have an adiabatic evolution of the propagating soliton pulse throughout the NLDC. The slow thermalization assumption arises from the consideration that we are interested in the investigation of coherent propagation and its limit of validity. Anyway, as far as the soliton area is in the stable region ($>\pi$), the area theorem guarantees a temporal reshaping that will reproduce a steady state, i.e., temporal broadening. A temporal change involves also the propagation velocity that in our case is critical for the efficiency of the exchange; therefore, fast relaxations compared to the time scale of the pulses may produce a pure depletion of the soliton structure. In the following we are going to show

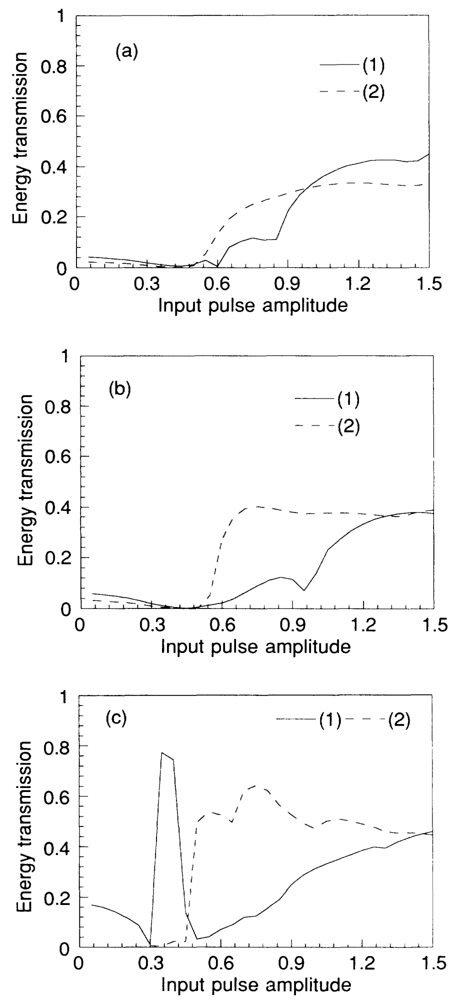

FIG. 7. Energy transmission normalized to the input energy as a function of the input amplitude A for the resonant case where dampings terms are included: (a) $\gamma'\tau'=0.1$, (b) $\gamma'\tau'=0.05$, and (c) $\gamma'\tau'=0.01$; the high extinction ratio is obtained only in the case of injected pulses much shorter than any relaxation time. This corresponds to the case (c) where the switching threshold is shifted towards smaller amplitudes compared to the threshold shown in Fig. 3. The pulse duration of the injected pulse is $\tau'=2$ and the coupler parameters are the same as those in Fig. 1.

the limits imposed by this phenomenon. By taking as an example the case of SIT propagation in bound excitons [11], the damping terms in the set of Maxwell-Bloch equations (15) are $\gamma_1^{-1}=135$ ps, $\gamma_2^{-1}=40-270$ ps, which are of the same order of magnitude, and the total broadening term is

$$\gamma_s^{-1}=(2\gamma_1+\gamma_2)^{-1}=25-54 \text{ ps} .$$

The pulse duration used in Sec. IV is $\tau'=2$, which in the case of bound excitons in CdS corresponds to $\tau=2$ ps and a product $0.04<\gamma_s\tau<0.08$. In this frame the effect of coherent loss is discussed. First, in Figs. 7 and 8, the energy transmission and the area curves concerning the case $\gamma'\tau'=0.1$ are shown, the injected pulse is a 2π soliton whose amplitude ranges from zero to $A=1.5$, and the pulse duration is $\tau'=2$. For amplitudes of the injected pulse in the range $0.6<A<0.85$, the propagation through the region of coupling determines complete switching, the energy left in the input waveguide is insufficient for another soliton formation, while in a coupled waveguide, a 2π soliton (with negative area) evolves keeping the area constant but not the amplitude. The latter decreases due to the incoherent processes and consequently a temporal adjustment of the pulse is required in order to keep the area constant. In fact, by numerically simulating the process, the output pulse is still a fundamental SIT soliton but is temporally broadened. In the range $0.9<A<1.4$, both channels support a 2π soliton and the associated energy transmission is about the same. Above $A=1.4$, again there is no contrast between the two channels, but the areas tend to switch to the 4π solution. For $\gamma'\tau'=0.05$, behavior is quite different; the transmission curves are reported in Figs. 7(b) and 8(b). From $A=0$ up to $A=0.9$, the input guide is lossy; the transmitted area associated to the propagating pulse is zero and the system behaves purely as an absorber. In the coupled waveguide, for $A<0.5$, no power is transmitted; beyond $A=0.5$, a fundamental SIT soliton is built and the correspondent energy transmission is about 40%: for $A>0.9$, the power injected in the input channel is sufficient for a 2π soliton formation that above $A=1.2$ is equally as intense as that in the coupled channel. In the case of $\gamma'\tau'=0.01$, the transition between the purely coherent propagation and the incoherent one is illustrated; the curves for the area and energy transmission evaluated at $\zeta_{\text{out}}=8$ are reported in Figs. 7(c) and 8(c). The energy transmission resembles that described in Fig. 3 for the resonant case, but the sharp power switching obtained at $A=0.5$ states a better performance of the device. The condition of $\gamma'\tau'=0.01$ states therefore an upper limit for coherent propagation without depletion. Whenever this condition is not satisfied, the initial pulse duration must be suitably reduced along with all the values of the parameters concerning coupler and doping.

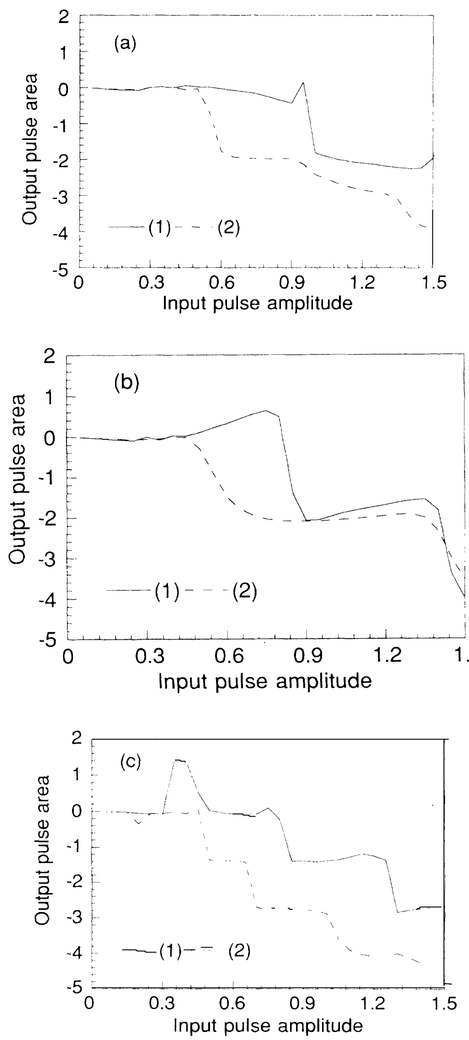

FIG. 8. Pulse area transmission as a function of the input amplitude A for the resonant case where dampings terms are included: (a) $\gamma'\tau'=0.1$, (b) $\gamma'\tau'=0.05$, and (c) $\gamma'\tau'=0.01$. The vertical axis is scaled in multiples of π.

VI. SOLITON COLLISION

An interesting situation is determined when two solitons travel separately along the two arms of the directional coupler. Hereafter, for the sake of simplicity, we will consider again the radiation in resonance with the two-level systems and pulses short enough to discard any relaxation time in the generalized Maxwell-Bloch equations (15). In this configuration we can distinguish two cases: one regards two equal input pulses shifted in phase by an arbitrary amount and another where the pulses differ in amplitude and duration but the initial phase and area are the same. In the following we discuss in more detail the former case. Starting from the particular configuration of two injected 2π pulses with the same amplitude, duration and phase, the last of the set of equations (15) reduces to

$$\frac{dU_1}{d\xi}=-\text{Im}P_1 ,$$

$$\frac{dU_2}{d\xi}=-\text{Im}P_2 ,$$

where $U_1=U_2$ are the envelopes of the fields relative to the two channels. This set represents the propagation of two independent pulses with no possibility of reciprocal interaction. The same consideration holds for any phase difference multiple of π; in general, if the initial conditions are symmetric or antisymmetric, the overall evolution remains unaffected by the coupling. On the contrary, when the input pulses have opposite quadratures, any symmetry consideration breaks up and coupling is allowed; in fact, Eqs. 15(b) become

$$\frac{d}{d\zeta}\mathrm{Re}U_1 = -\mathrm{Im}P_1 \pm K\,\mathrm{Im}U_2 ,$$

$$\frac{d}{d\zeta}\mathrm{Im}U_2 = -\mathrm{Re}P_2 \mp K\,\mathrm{Re}U_1 .$$

The signs in front of the coupling constant K refer to a $\pm\pi/2$ relative phase shift between the input fields. But, as already discussed in Sec. III, for having a substantial energy exchange the injected fields or areas must be large enough or the pulse has to be short in duration in order to overcome the pure soliton propagation originating from the polarization source terms $\mathrm{Im}U_1$ and $\mathrm{Re}U_2$. In any case, if the linear coupling prevails, the system describes a case of directional coupling with two fields as initial condition, and its solution is a superposition of solutions of the case of a single input field [12] having opposite quadratures. The resulting expressions read

$$\mathrm{Re}U_1(z) = \mathrm{Re}U_1(0)[-\sin(K\zeta) \mp \cos(K\zeta)] ,$$

$$\mathrm{Im}U_2(z) = \mathrm{Im}U_2(0)[\mp\sin(K\zeta) + \cos(K\zeta)] .$$

For the power transmission we obtain

$$P_1(\zeta) = P_1(0)[1 \pm \sin(2K\zeta)]$$

and

$$P_2(\zeta) = P_2(0)[1 \mp \sin(2K\zeta)] ;$$

the opposite order for the signs in the two expressions always refers to the sign of the initial phase shift. The power evolutions indicate that after a coupling distance $\zeta = \pi/(2K)$, the total power is recovered into one of the two waveguides constituting the device and the choice of the output port depends on the sign of the initial phase difference between the fields. In general, it is worthwhile to note that either for integer or semi-integer multiples of π, only one of the two quadratures of each field has been used; this means that fields traveling in the two waveguides do not suffer further phase shifts besides the initial one. This description constitutes only a simple qualitative approach to the problem. On the contrary, when the initial phase shift is an arbitrary angle, the four quadratures contained in Eqs. (15) are involved; in this configuration it is possible to have a case in which there exists a competition between the pure SIT soliton propagation (as the two waveguides were separated) and the linear coupling effect that produces a transfer of energy from one of the two arms to the other (depending on the sign of the perturbation). In Fig. 9 we examine the evolution of two equal pulses shifted in phase by $\pi/20$ launched into the input ports of the directional coupler for three different input powers: the input pulses correspond to two equal pulses whose duration $\tau'=2$; since the pulses are equal, the envelope velocities are equal too and therefore the coupling region may be located in any point of the device. In Fig. 9(a), we compare the plots of energy (N) versus distance of the two traveling pulses; the amplitudes of the identical pulses are chosen in order to have two areas of 1.8π ($N=0.81$) each. In the simulation, the phase-shifted pulse propagating through the coupler switches to the crossed waveguide, adding its energy to the unshifted pulse (if the relative phase difference were reversed, the effect would be the opposite); these results suggest that the linear part is predominant. In Fig.

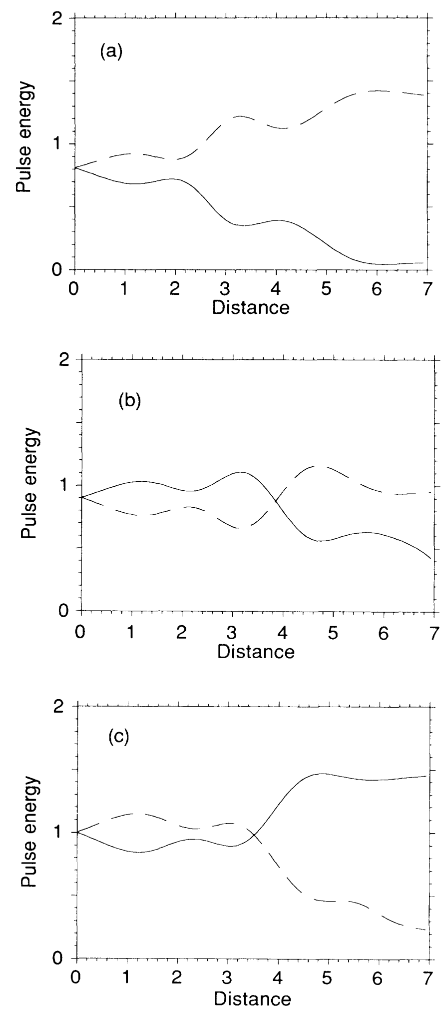

FIG. 9. Collision of SIT solitons. Plot of the pulse energies N vs distance ζ of a pair of 2π pulses injected into the two arms of the directional coupler, one for each waveguide; the energy evolution corresponding to the dashed line refers to the $\pi/20$ phase-shifted input field: The normalized coupling constant is $K=2$, the coupling length is $d=2$, and the coupler position is $\zeta_m=2.5$. In (a) the input areas are set at 1.8π ($A=0.45$, $\tau'=2$); the coupler behaves linearly. In (b) the areas are set at 1.9π ($A=0.475$, $\tau'=2$); both channels transmit energy and the one that previously was lossy now is favored. In (c) the input areas are set equal to 2π ($A=0.5$, $\tau'=2$); the outport inversion with respect to the case (a) is evident.

9(b), the input areas have been increased to 1.9π ($N=0.9025$), while the pulse durations have been kept constant; this is an intermediate case in which both the waveguides transmit power and the previously lossy channel now contains a sufficient amount of energy to form a SIT soliton, while the other channel that at $\zeta_{out}=8$ still guides energy shows a trend to complete depletion. In between 1.8π and 1.9π, there exists a threshold for the change in direction of coupling that becomes completely defined by raising the input areas to 2π in each waveguide ($N=1$); this case is reported in Fig. 9(c) which compared to Fig. 9(a), depicts just the opposite evolutions for the energies flowing through the two channels. In the three cases illustrated in Fig. 9, only the input area has been changed and around a certain value of it the transmission of the directional coupler may change quite a lot; this may be surprising, but a small change of initial conditions—the amplitudes in the present case—determine a substantial variation of the absolute phase relative to each pulse during the propagation and, as seen above, a change in the sign of the phase difference determines a change in the outport too. Therefore, the effect of outport switching seems to be a consequence of the constructive or destructive interference of the fields coupled to the two waveguides and when the propagating pulse area decreases below the threshold for soliton formation, the pulse undergoes pure absorption. An analogous mechanism for SIT soliton switching through a collision process holds even when two equally phased solitons different in amplitude and duration but with same area are separately injected into the two arms of the directional coupler. From the last of Eqs. (15) we have that when the two input pulses are different in amplitude and correspondingly in duration they are not independent anymore, even though the initial phases are the same; this can be easily derived by decomposing the fields appearing in the last of Eqs. (15) in amplitudes and phases ($|U_j|,\phi_j$): once the phases of each pulse may evolve along the waveguides, the same process described above may occur. In Fig. 10 we report the plots of the energy evolution $N=N(\zeta)$ through the coupler of a pair of 2π solitons whose amplitudes and durations are $A_1=0.5$, $\tau_1'=2$, $A_2=0.25$, and $\tau_2'=4$, and in Fig. 11 we report the space-time maps of this interaction. Since the two SIT solitons travel with different envelope velocity, for the faster pulse we chose a starting time $t_0'=-8$ with respect to that of the slower one in order to allow the collision just in the center of the coupling region that was posi-

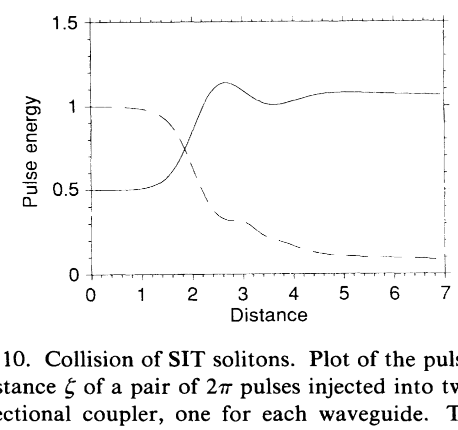

FIG. 10. Collision of SIT solitons. Plot of the pulse energies N vs distance ζ of a pair of 2π pulses injected into two arms of the directional coupler, one for each waveguide. The energy evolution corresponding to the solid line corresponds to an input pulse whose amplitude is $A=0.5$ and whose duration $\tau'=2$, while that corresponding to the dashed line is for $A=0.25$ and $\tau'=4$. Here the input phases are the same; the timing for the injection was $t_{01}'=0$ for the slower pulse and $t_{02}'=-8$ for the faster one. The set of parameters for the coupler is the same as that of Fig. 9. Around the coupling region the energy of the short pulse switches completely to the opposite channel.

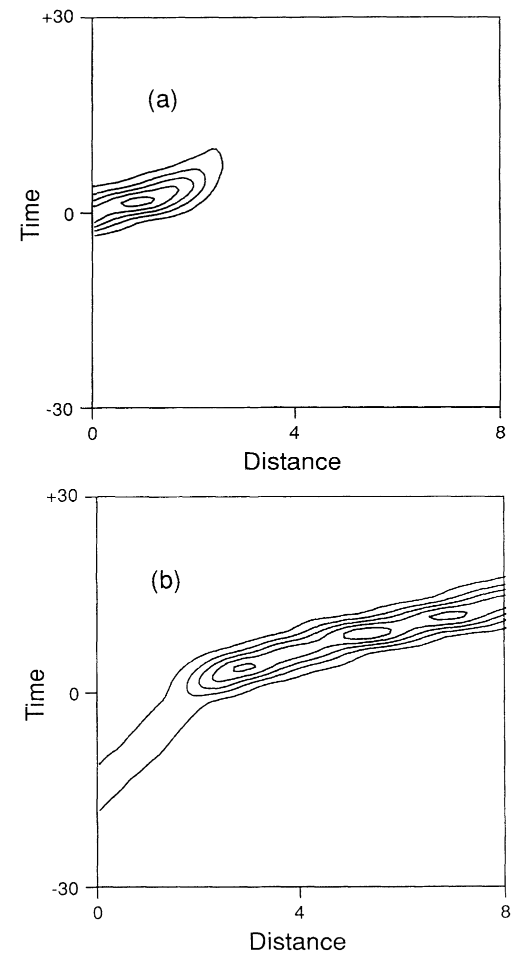

FIG. 11. Collision of SIT solitons. Space-time maps relative to the case reported in Fig. 10. The horizontal axis is the propagation distance ζ, while the vertical axis is the time t': The maps are represented in the reference frame of the speed of light; therefore, the horizontal scale corresponds to a pulse traveling at the speed of light. The faster pulse starts delayed with respect to the slow one in order to collide in the region of coupling; after the collision the total energy is collected in the channel corresponding to the slow pulse. Once the superposition has occurred, the resulting envelope undergoes a reshaping that gives rise to a shorter pulse whose velocity is close to that of the light. In (a) the map corresponding to the channel where the fast pulse is launched is reported and in (b), the map corresponding to the channel where the slow pulse is launched.

tioned at $\zeta_m = 2.5$. The choice of the above parameters for the two SIT solitons was dictated by the fact that if they traveled by themselves without interacting, they would not switch [as illustrated in cases (a) and (b) of Figs. 1 and 2]; in the present configuration, instead, the faster pulse (labeled 1) switches completely to the opposite channel, adding energy to the slower pulse which after a sudden reshaping acquires speed and keeps traveling at a velocity close to that of the faster one. The collision of two different SIT solitons constitutes another way to control light with light and most likely is more convenient because it does not require a strict control of the phases of the incoming pulses.

VII. CONCLUSION

A type of nonlinear directional coupler has been presented. In analogy with the Kerr soliton directional coupler, this shows a power-dependent transmission; on the contrary, the basic mechanisms of the two switches differ in the sense that the Kerr one works on a change of phase velocity, the coherent one on a change of the pulse group velocity. When the pulse carrier frequency is resonant with the transition of the two-level system, the equations for coherent propagation show that the fundamental 2π SIT soliton travels unperturbed along the input channel of the directional coupler and therefore linear coupling is inhibited, while the second-order 4π soliton switches into crossed channel. The transition from inhibition to exchange is well defined and occurs for an injected pulse area corresponding to the second instability point of the area theorem diagram, i.e., around 3π. The higher-order injected solitons, during propagation through the coupling region, split up in integer multiples of the fundamental one and occupy both channels of the device. This indicates that the overall transmission of the device is digital. This means that a single SIT soliton never shares its area or energy between the two channels, but maintains at least its fundamental unit in one channel. The study has also been extended to the off-resonance case. In this configuration small detunings still allow the velocity-group-based mechanism of switching while large detunings transform the interaction in the Kerr type (phase-velocity dependence on power) and, in this case, a much higher input power would be required to obtain switching [5]. The damping terms as longitudinal and transverse relaxation rates were taken into consideration too. The effect of those may dramatically reduce the nonlinear efficiency of the device. Therefore very short pulses are required, that is, in the direction of ultra high-bit-rate-based telecommunication networks. In this area of interest it may be useful to govern the switching process through a mechanism of control. In this sense we observed that when two fundamental SIT's travel separately along the two arms of the directional device and are weakly shifted in phase one from the other, there is an area threshold which allows even in this case the choice of the output port. In analogy to this case, the mechanism of nonlinear-phase-based switching applies when two 2π solitons different in amplitude and duration are injected in the two arms of the directional coupler, giving rise again to an outport switching controlled by an external pulse. In conclusion, since the SIT nonlinear directional coupler operates on the principle of self-induced transparency, the maximum nonlinearity attainable from a two-level system is used and at the same time the contribution of the absorption losses is largely reduced.

ACKNOWLEDGMENTS

M.R. is pleased to acknowledge financial support from the ICFES-BID program. F.S.L., M.R., and S.W. carried out this work in the framework of the agreement between Fondazione U. Bordoni and the Istituto Superiore delle Poste e Telecomunicazioni and with partial financial support from Italian National Research Council (CNR).

[1] S. M. Jensen, IEEE J. Quantum Electron. **QE-18**, 1580 (1982); B. Daino, G. Gregori, and S. Wabnitz, J. Appl. Phys. **58**, 4512 (1985); H. G. Winful, Appl. Phys. Lett. **47**, 213 (1985); S. Trillo, S. Wabnitz, N. Finlayson, W. C. Banyai, C. T. Seaton, G. I. Stegeman, and R. H. Stolen, *ibid.* **53**, 837 (1988); S. R. Friberg, A. M. Weiner, Y. Silberberg, B. G. Sfez, and P. W. Smith, Opt. Lett. **13**, 904 (1988).

[2] A. Hasegawa and F. Tappert, Appl. Phys. Lett. **23**, 142 (1973).

[3] K. J. Blow, N. J. Doran, and B. K. Nayar, Opt. Lett. **14**, 754 (1989); M. N. Islam, E. R. Sunderman, R. H. Stolen, W. Pleibel, and J. R. Simpson, *ibid.* **14**, 811 (1989).

[4] S. Trillo, S. Wabnitz, E. M. Wright, and G. I. Stegeman, Opt. Lett. **13**, 672 (1988).

[5] G. I. Stegeman, C. Seaton, A. C. Walker, and C. N. Ironside, Opt. Commun. **61**, 277 (1987); R. Jin, C. L. Chuang, H. M. Gibbs, S. W. Koch, J. N. Polky, and G. A. Pubanz, Appl. Phys. Lett. **53**, 1791 (1981); R. Jin, C. L. Chuang, H. M. Gibbs, S. W. Koch, J. N. Polky, and G. A. Pubanz, Appl. Phys. Lett. **53**, 1791 (1988); D. Hulin, A. Mysyrowicz, A. Antonetti, A. Migus, W. T. Masselink, H. Morkoc, H. M. Gibbs, and N. Peyghambarian, Appl. Phys. Lett. **49**, 749 (1986).

[6] S. L. McCall and E. L. Hahn, Phys. Rev. Lett. **18**, 908 (1967); Phys. Rev. **183**, 457 (1969).

[7] A. Guzman, M. Romagnoli, and S. Wabnitz, Appl. Phys. Lett. **56**, 614 (1990).

[8] C. K. Rhode and A. Szoke, Phys. Rev. **184**, 25 (1969); F. M. Mattar and M. C. Newstein, J. Quantum Electron. **QE-13**, 507 (1977).

[9] V. M. Agranovich, V. Y. Chernyak, and V. I. Rupasov, Opt. Commun. **37**, 363 (1981).

[10] M. Romagnoli, S. Wabnitz, and L. Zoccolotti, Opt. Lett. **16**, 1249 (1991).

[11] K. Watanabe, H. Nukono, A. Honold, and Y. Yamamoto, Phys. Rev. Lett. **62**, 2257 (1989).

[12] See, for example, A. Yariv, *Quantum Electronics,* 3rd ed. (Wiley, New York, 1989).

[13] U. Langbein, F. Lederer, and H. E. Ponath, Opt. Quantum Electron. **16**, 251 (1984).

[14] H. M. Gibbs and R. E. Slusher, Phys. Rev. A **6**, 2326 (1972).